JCB Article

VCIP135, a novel essential factor for p97/p47-mediated membrane fusion, is required for Golgi and ER assembly in vivo

Keiji Uchiyama,[1] Eija Jokitalo,[2] Fumi Kano,[3] Masayuki Murata,[3] Xiaodong Zhang,[4] Benito Canas,[5] Richard Newman,[6] Catherine Rabouille,[7] Darryl Pappin,[5] Paul Freemont,[4] and Hisao Kondo[1,8]

[1]Cambridge Institute for Medical Research, University of Cambridge, Cambridge CB2 2XY, United Kingdom
[2]Institute of Biotechnology, University of Helsinki, Helsinki FIN-00014, Finland
[3]National Institute for Physiological Sciences, Okazaki 444-8585, Japan
[4]Centre for Structural Biology, Imperial College of Science, Technology and Medicine, London SW7 2AZ, United Kingdom
[5]Clinical Pharmacology, Imperial College School of Medicine, London W12 0NN, United Kingdom
[6]European Molecular Biology Laboratory-European Bioinformatics Institute, Cambridge CB10 1SD, United Kingdom
[7]University Medical Centre Utrecht, Academic Ziekhuis Utrecht, 3584CX Utrecht, Netherlands
[8]PREST and SORST, Japan Science and Technology Corporation, Saitama 332-0012, Japan

NSF and p97 are ATPases required for the heterotypic fusion of transport vesicles with their target membranes and the homotypic fusion of organelles. NSF uses ATP hydrolysis to dissociate NSF/SNAPs/SNAREs complexes, separating the v- and t-SNAREs, which are then primed for subsequent rounds of fusion. In contrast, p97 does not dissociate the p97/p47/SNARE complex even in the presence of ATP. Now we have identified a novel essential factor for p97/p47-mediated membrane fusion, named VCIP135 (valosin-containing protein [VCP][p97]/p47 complex-interacting protein, p135), and show that it binds to the p97/p47/syntaxin5 complex and dissociates it via p97 catalyzed ATP hydrolysis. In living cells, VCIP135 and p47 are shown to function in Golgi and ER assembly.

Introduction

The Golgi apparatus plays a central role in intracellular membrane traffic. It undergoes dramatic transformation during the cell cycle (Warren, 1993). During mitosis, it is fragmented into thousands of vesicles and short tubules that are dispersed throughout the cytoplasm. Some or all of them might be absorbed into ER, which is still a matter of controversy (Zaal et al., 1999; Jokitalo et al., 2001; Check, 2002). At telophase, the mother cell divides into two daughter cells, and a Golgi apparatus is rapidly reassembled from fragments within each daughter cell (Lucocq et al., 1989). Experiments using an in vitro Golgi reassembly assay showed that reassembly from membrane fragments requires at least two ATPases: NSF and p97 (also known as valosin-containing protein [VCP]*) (Rabouille et al., 1995b). The mechanism of action of NSF in mediating membrane fusion has been the subject of a considerable amount of work, and its role has been well characterized. In contrast to NSF, much less is known about the mechanism of action of p97. Only one cofactor has so far been identified, namely p47. It forms a tight complex with p97, which is essential for the in vitro Golgi reassembly (Kondo et al., 1997). The SNARE protein, syntaxin5, is a receptor in Golgi membranes for the p97/p47 complex with p47 mediating the binding of p97 to syntaxin5 (Rabouille et al., 1998).

NSF binds to SNAREs via α-SNAP and dissociates the resulting complex using ATP hydrolysis (Sollner et al., 1993). The SNAREs are thought to be activated ("primed") in the process of the complex dissociation (Wickner and Haas, 2000). These primed SNAREs are

The online version of this article contains supplemental material.

Address correspondence to Hisao Kondo, Cambridge Institute for Medical Research, Rm 5.36, University of Cambridge, Wellcome Trust/MRC Bldg., Hills Rd., Cambridge CB2 2XY, UK. Tel.: 44-1223-762632. Fax: 44-1223-762640. E-mail: hk228@cam.ac.uk

E. Jokitalo and F. Kano contributed equally to this work.

Key words: membrane fusion; p97; VCIP135; Golgi; ER

*Abbreviations used in this paper: GalT, β1,4-galactosyltransferase; PDI, protein disulfide isomerase; SAND, sulfosuccinimidyl 2-[*m*-azido-*o*-nitrobenzamido]ethyl-1,3′-dithiopropionate; VCIP135, VCP(p97)/p47 complex-interacting protein, p135; VCP, valosin-containing protein.

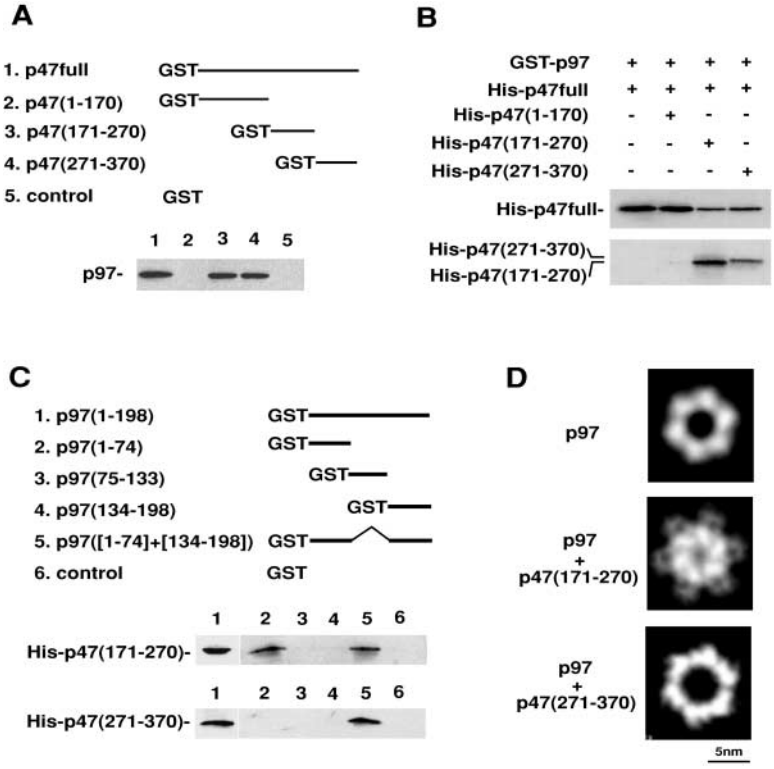

Figure 1. **Two distinct binding interactions in the p97/p47 complex.** (A) Each GST-tagged deletion mutant of p47 was incubated with p97 in a buffer containing 0.1% Triton X-100 on ice, then isolated on glutathione beads, and bound proteins were fractionated by SDS-PAGE. Blots were probed with anti-p97 antibodies. (B) GST-tagged p97 (1.5 μg) was incubated with p47full (0.5 μg) either alone or in combination with a deletion mutant of p47 (4 μg) on ice. Blots were probed with antibodies to the His-tag on p47 fragments. (C) GST-tagged deletion mutants of p97 were incubated with each of the p47 fragments containing the p97-binding sites on ice. Blots were probed with antibodies to the His tag on the p47 fragments. (D) p97 was preincubated with an excess amount of p47 fragments containing the p97-binding sites and purified by gel filtration followed by EM observation.

then available to pair with SNAREs in other membranes, thereby inducing further rounds of fusion. Similar to NSF, p97 is also thought to prime SNAREs via ATP hydrolysis, though in this instance only t-SNAREs appear to be involved and the mechanism of priming is unclear. In previously reported experiments, we isolated a p97/p47/syntaxin5 complex and visualized it by EM (Rabouille et al., 1998). Surprisingly, this complex was observed even in the presence of ATP. Unlike NSF, p97 appears not to dissociate the p97/p47/syntaxin5 complex. Therefore, how does the p97/p47 complex prime SNAREs? Is another unidentified factor required for the dissociation of the p97/p47/SNARE complex?

Another important question with respect to p97 and its yeast homologue, Cdc48p, is whether it is really necessary for membrane fusion in vivo. Several groups have reported on its membrane fusion activity in different in vitro assay systems (Acharya et al., 1995; Latterich et al., 1995; Rabouille et al., 1995b; Roy et al., 2000; Hetzer et al., 2001), but there is no direct evidence concerning its in vivo function. In addition, several functions of p97/Cdc48p in other biological pathways have been reported apart from its action in membrane fusion (Patel and Latterich, 1998; Meyer et al., 2000; Dai and Li, 2001; Ye et al., 2001; Jarosch et al., 2002), and the lack of evidence about its membrane fusion activity in vivo has caused much confusion and controversy.

In this paper, we have resolved some of these arguments. We identified VCIP135 (VCP[p97]/p47 complex-interacting protein, p135), a novel essential factor for p97/p47-mediated membrane fusion and showed that it binds to the p97/p47/syntaxin5 complex and dissociates it via p97 catalyzed ATP hydrolysis. In addition, by microinjection of antibodies to VCIP135 and p47 into living cells we have succeeded in clarifying that VCIP135 and p47 are required for Golgi assembly and ER network formation in vivo.

Results

Two binding interactions in the p97/p47 complex

To determine the p97-binding sites on p47, we prepared several GST-tagged deletion mutants of p47 and checked their ability to bind to p97 (Fig. 1 A). p47(171–270) and p47(271–370) bind to p97, but p47(1–170) does not, suggesting the existence of two p97-binding sites on p47. This was confirmed by competition experiments between full-length p47 (p47full) and p47 fragments (Fig. 1 B). p47(171–270) and p47(271–370) inhibit the binding of p47full to p97, but p47(1–170) does not. Since p47full binds to the NH_2-terminal domain of p97 (unpublished data), more detailed mapping of the p47-binding sites in p97 was performed (Fig. 1 C). The two p47 fragments showed different binding properties to p97. Although a single NH_2-terminal domain of p97(1–74) was sufficient for p47(171–270) binding (Fig. 1 C, top), both p97 NH_2-terminal domains, p97(1–74) and p97(134–198), were necessary for p47(271–370) binding (Fig. 1 C, bottom).

To characterize further the binding, EM of negatively stained complexes of p97/p47 fragments was performed. As shown in Fig. 1 D, the averaged projection images of the resultant complexes were different to that of p97 alone. Since the sizes of the p47 fragments are too small (~10 kD) to allow direct observation by EM, the observed changes in the EM images largely represent conformational changes in p97. These observations therefore suggest that p97 undergoes significant conformational changes upon p47 fragment bind-

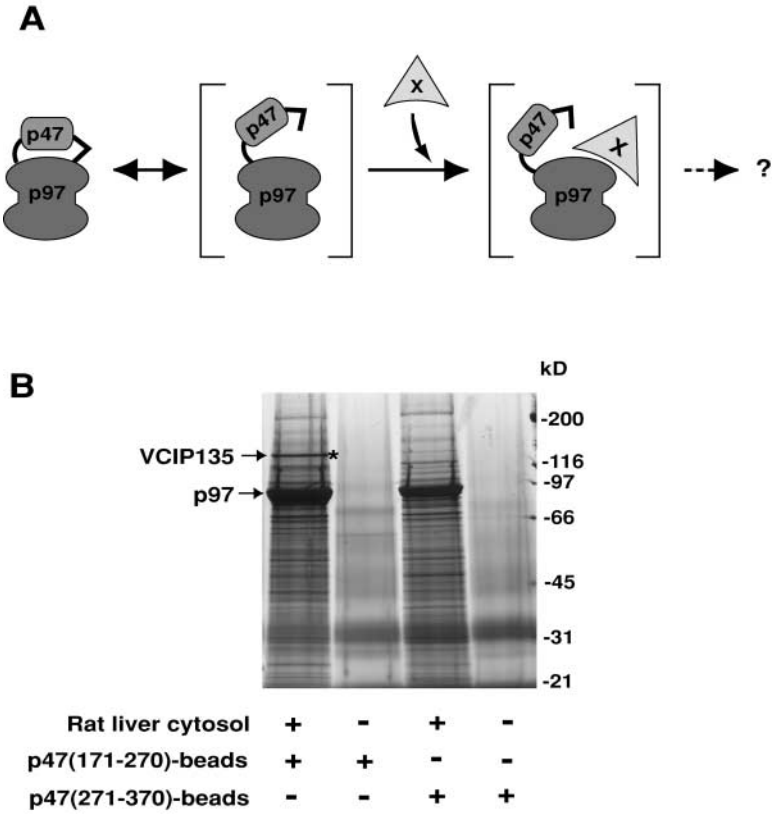

Figure 2. **Identification of VCIP135.** (A) A working model of how a p97/p47-interacting protein (protein X) forms an unstable ternary complex with p97 and p47. (B) Purification of VCIP135 from rat liver cytosol. Each small p47 fragment with a p97-binding site was immobilized on beads and incubated with rat liver cytosol. Bound proteins were eluted by a 1 M KCl wash, TCA-precipitated, fractionated, and silver stained. VCIP135 was isolated on p47(171–270) beads (asterisk).

ing. In summary, our data show that p47 and p97 have two distinct binding interactions.

Identification of VCIP135 as a p97/p47 complex–interacting protein

We first tried to isolate a p97/p47-interacting protein using p47full beads but could only isolate p97 (unpublished data). This suggested that an interacting protein, even if it existed, might form an unstable ternary complex with p97 and p47. The existence of two distinct p97/p47 binding interactions could result in transient or unstable complexes that use only one p97/p47 binding interaction (Fig. 2 A). Based on the idea that such unstable p97/p47 complexes could be a target for an interacting protein X, we next tried to isolate such a protein using small p47 fragments containing only one of the p97-binding sites as bait. The p47 fragments were immobilized on beads, mixed with rat liver cytosol, and bound proteins were analyzed. The results are shown in Fig. 2 B. As expected, both p47 fragments bound to p97. Interestingly, another protein of 135kD (VCIP135) was isolated only using p47(171–270) beads (Fig. 2 B, asterisk). After Zn-staining, this protein band was excised from the gel and subjected to protein microsequencing by electrospray mass spectrometry. We obtained two partial peptide sequences that allowed us to clone a novel cDNA sequence corresponding to VCIP135. Its nucleotide sequence are available from the DNA data bank of Japan database under the accession no. AB045378. Kazusa DNA Research Group also reported the cDNA sequence of its human homologue (Nagase et al., 2001). Western blotting using anti-VCIP135 antibodies showed that it was widely expressed all over the rat tissues (unpublished data).

VCIP135 dissociates the p97/p47 complex through p97 ATP hydrolysis

To characterize the interactions between VCIP135 and the p97/p47 complex, detailed immunoprecipitation experiments were performed. As shown in Fig. 3 A, anti-VCIP135 antibodies coimmunoprecipitated a protein of 97 kD from the cytosol (left), which was shown to be p97 by Western blotting (right middle). However, p47 could not be detected in these precipitates (Fig. 3 A, right bottom). These data indicate that VCIP135 can form a stable complex with p97 in cytosol and that p47 is not part of this complex. As presented in Fig. 3 B, the fractionation of cytosol by sucrose-gradient sedimentation showed that VCIP135 distributed in lighter fractions (lanes 3–6) and in the p97-containing fractions (lanes 7–10), suggesting the existence of two populations of cytosolic VCIP135: one in complex with p97 and the other free of p97.

We then mapped the interaction between VCIP135 and p97, the results of which are shown in Fig. 3 C (see also Fig. S1 available at http://www.jcb.org/cgi/content/full/jcb.200208112/DC1). Various truncated His tag VCIP135 fragments were tested for their ability to bind p97. The COOH-terminal region of VCIP135 (744–1221) proved to be important for p97 binding (Fig. 3 C, lane 3). Interestingly, fold recognition analysis of VCIP135 identified a region between residues 744 and 860 to have a similar fold to SUMO-1 (Bayer et al., 1998), suggesting a ubiquitin-like structure for this part of VCIP135. Recently, a nuclear magnetic resonance spectroscopy study has shown that the p47 COOH-terminal domain (residues 270–370) is also a ubiquitin-like domain and that this region specifically binds to the NH_2-terminal domain of p97 (Yuan et al., 2001). It is

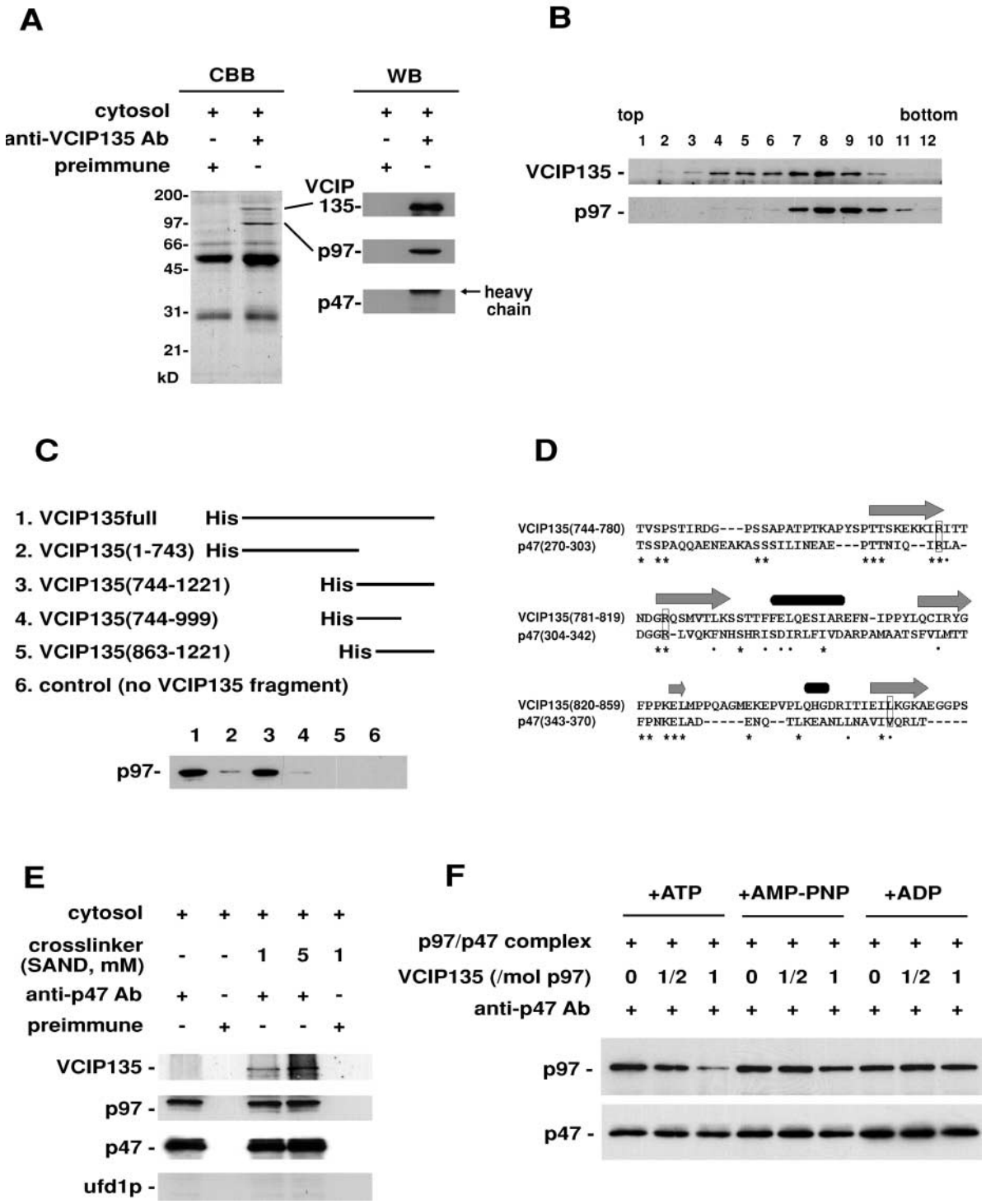

Figure 3. **VCIP135 binds to and dissociates the p97/p47 complex.** (A) Rat liver cytosol (3.5 mg total protein) was incubated with preimmune serum or anti-VCIP135 antibodies. The immunoprecipitates were fractionated by SDS-PAGE followed by staining with Coomassie blue (CBB, left) and Western blotting with antibodies to VCIP135, p97, and p47 (WB, right). (B) Rat liver cytosol was size fractionated by 5–30% sucrose sedimentation, and the fractions were assayed by Western blotting with antibodies to VCIP135 and p97. (C) His-tagged deletion mutants of VCIP135 were incubated with p97 in a buffer containing 0.1% Triton X-100 on ice and then precipitated by anti–His tag antibodies. Blots were probed with anti-p97 antibodies. (D) The sequence alignment between VCIP135(744–859) and p47(270–370). Identical (asterisk) and conserved residues (□) are marked. Arrows and black bars show β-strands and α-helices, respectively. The three surface residues identified as potential p97-interacting residues in p47 are boxed (Yuan et al., 2001) and are conserved in VCIP135. (E) Rat liver cytosol (3.5 mg total protein) was cross-linked with SAND and incubated with preimmune serum or anti-p47 antibodies. The immunoprecipitates were fractionated by SDS-PAGE followed by Western blotting with antibodies to VCIP135, p97, p47, and Ufd1p (a negative control). (F) p97 was incubated with an excess amount of p47, and the p97/p47 complex was purified using gel filtration in the absence of nucleotides. The purified p97/p47 complex (1.2 μg p97) was incubated in a buffer (50 μl) containing 1 mM nucleotide on ice for 30 min. VCIP135 (0.8 or 1.6 μg) was added into the mixture and incubated on ice for 1 h, and p97 that formed a complex with p47 was coimmunoprecipitated with anti p47 antibodies. Blots were probed with antibodies to p97 and p47.

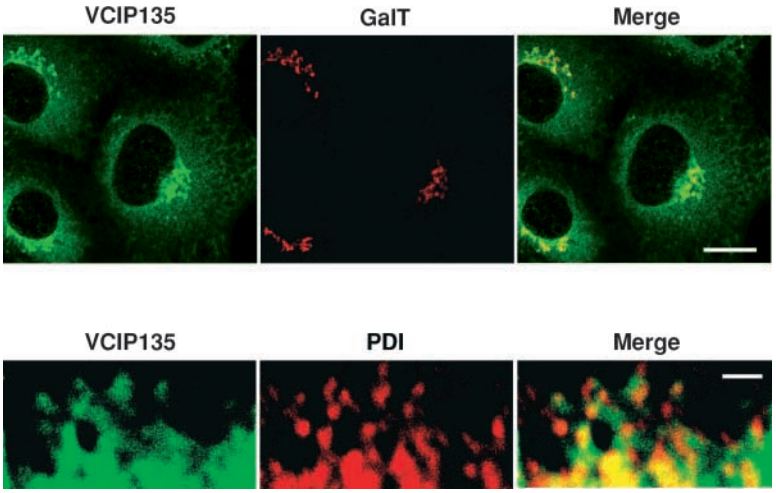

Figure 4. **The localization of VCIP135.** Double immunofluorescence staining of VCIP135 and either GalT, a Golgi marker, or PDI, an ER marker, shows that VCIP135 localizes to Golgi and ER. NRK cells were fixed by methanol at −20°C for 4 min, stained with antibodies, and observed by confocal microscopy. Bars: (top) 10 μm; (bottom) 2 μm.

therefore plausible that both VCIP135 and p47 use homologous ubiquitin-like domains (Fig. 3 D) to bind to the same region of p97, suggesting that p47(271–370) competes with VCIP135 for p97 binding. This provides a reasonable explanation for our biochemical data that p47(271–370) binds to p97 but not to the p97/VCIP135 complex (Fig. 2 B).

We originally isolated VCIP135 as a candidate p97/p47-interacting protein and thus needed to establish whether it can form a complex with p97/p47. As discussed in the previous section, a ternary complex of p97/p47/VCIP135 might be unstable, and hence, we used a cross-linker reagent to capture it. Coimmunoprecipitation experiments were performed in the presence of the cross-linker, sulfosuccinimidyl 2-[*m*-azio-*o*-nitrobenzamido]ethyl-1,3′-dithiopropionate (SAND) (Fig. 3 E). VCIP135 was coimmunoprecipitated by anti-p47 antibodies only in the presence of SAND (Fig. 3 E, lanes 3 and 4) but not in its absence (lane 1). The preimmune serum did not coimmunoprecipitate any VCIP135 even in the presence of SAND (Fig. 3 E, lane 5). ufd1p, a negative control, was not precipitated in any lanes (bottom). Hence, VCIP135 could bind to the p97/p47 complex in cytosol, possibly forming an unstable complex of p47, p97, and VCIP135 that was captured after chemical cross-linking. This led to the question of what effect VCIP135 would have on the p97/p47 complex after forming the unstable ternary complex.

To answer this question, VCIP135 was added to the purified p97/p47 complex in the presence of nucleotides (Fig. 3 F). After incubation, the p97 bound to p47 was coimmunoprecipitated by anti-p47 antibodies in order to separate it from the p97 bound to VCIP135. In the presence of ATP, VCIP135 dissociated the p97/p47 complex in a dose-dependent manner (Fig. 3 F, left three lanes). In the presence of AMP–PNP, a nonhydrolyzable ATP analogue, or ADP, the dissociation of the complex was not observed (Fig. 3 F, the middle and right three lanes, respectively), indicating that dissociation of p97/p47 complex by VCIP135 required ATP hydrolysis. Together these data show that VCIP135 interacts with the p97/p47 complex and dissociates it as a consequence of ATP hydrolysis by p97.

VCIP135 dissociates the p97/p47/syntaxin5 complex

Although VCIP135 was originally purified from cytosol, it is also localized to Golgi and ER. As presented in Fig. 4, double immunofluorescence staining of VCIP135 and either β1,4-galactosyltransferase (GalT), a Golgi marker, or protein disulfide isomerase (PDI), an ER marker, showed localization to Golgi and ER.

Syntaxin5 is a SNARE in both the Golgi and ER (Hui et al., 1997) and has been shown to be involved in the p97/p47 fusion pathway (Rabouille et al., 1998). Hence, we investigated the interaction between VCIP135 and syntaxin5 by binding experiments using GST-tagged syntaxin5 without the transmembrane domain (GST–syn5ΔTM) as shown in Fig. 5 A. Since syntaxin1 is a SNARE in plasma membranes, we used GST–syn1ΔTM as a negative control. We found that GST–syn5ΔTM bound VCIP135 very efficiently (Fig. 5 A, lane 1) compared with GST–syn1ΔTM (lane 2). The specificity of binding of VCIP135 to syntaxin5 was further confirmed by the coimmunoprecipitation experiments using Golgi membranes as shown in Fig. 5 B. 1 M KCl-washed Golgi membranes were incubated with His-tagged VCIP135. After removing unbound VCIP135, the membranes were solubilized and VCIP135, and its binding proteins were immunoprecipitated by antibodies to the His tag on VCIP135. Syntaxin5 was coimmunoprecipitated (Fig. 5 B), providing evidence that VCIP135 binds to syntaxin5 in Golgi membranes.

We next incubated VCIP135 and GST–syn5ΔTM together with p97 and p47 in the absence of nucleotides and then isolated the proteins bound to GST–syn5ΔTM (Fig. 5 C). VCIP135 bound to GST–syn5ΔTM either with p47 or p97/p47 (Fig. 5 C, lanes 5 and 6, respectively). This simple binding experiment showed that VCIP135 can form a quaternary complex with syntaxin5, p97, and p47 (Fig. S2 available at http://www.jcb.org/cgi/content/full/jcb.200208112/DC1). VCIP135 did not bind to syntaxin5 with p97 (Fig. 5 C, lane 4), a finding which was investigated further (Fig. 5 F).

A further question is what are the consequences of the ATP hydrolysis by p97 on the quaternary complex of VCIP135/p97/p47/syntaxin5? To address this, we first performed binding experiments: p97/p47 was incubated with either GST–syn5ΔTM or VCIP135 + GST–syn5ΔTM in the presence of nucleotides, and the proteins bound to GST–syn5ΔTM were analyzed (Fig. 5 D; see also Fig. S3 available at http://www.jcb.org/cgi/content/full/jcb.200208112/

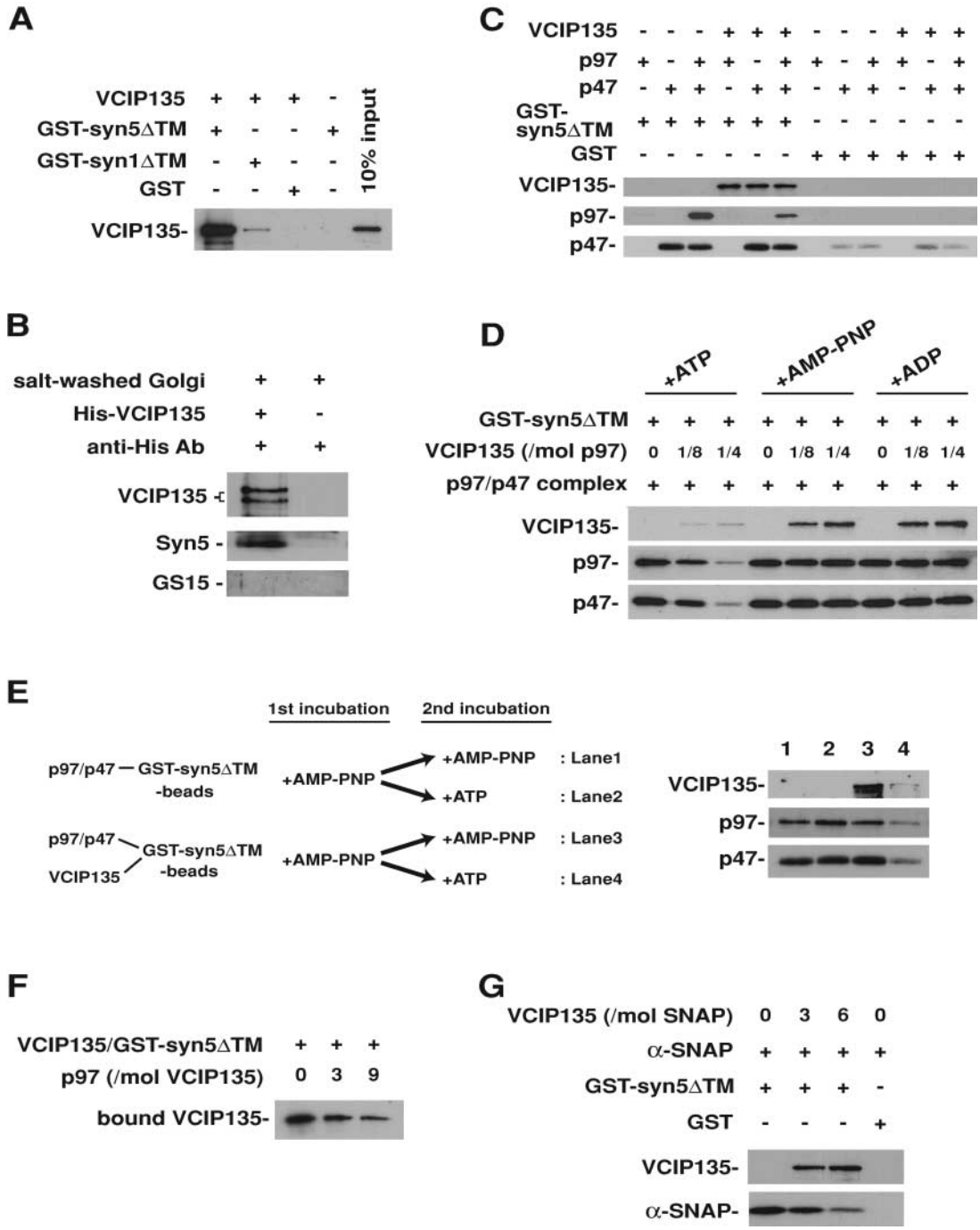

Figure 5. **VCIP135 binds to syntaxin5 and dissociates the p97/p47/syntaxin5 complex via p97 catalyzed ATP hydrolysis.** (A) His-tagged VCIP135 (0.4 μg) was incubated with either GST, GST–syn5ΔTM, or GST–syn1ΔTM (0.5 μg each) in a buffer (50 μl) containing 0.1% deoxycholate on ice and isolated on glutathione beads. Blots were probed with antibodies to VCIP135. (B) 1 M KCl-washed Golgi membranes were incubated with His-tagged VCIP135 on ice for 1 h. The membranes were isolated from unbound VCIP135 by centrifugation and solubilized in a buffer containing 1% CHAPS. VCIP135 and its interacting proteins were immunoprecipitated by mAbs to the His tag on VCIP135 and fractionated by SDS-PAGE followed by Western blotting with antibodies to syntaxin5 peptide, VCIP135, and GS15 (a negative control). The bottom band of VCIP135 is a degradative product. (C) GST–syn5ΔTM (0.5 μg) or GST (0.5 μg) was incubated with p97 (2 μg), p47 (1 μg), VCIP135 (3 μg), or their combinations in 50 μl of buffer containing 0.1% deoxycholate, but no nucleotide on ice, and isolated on glutathione beads. Blots were probed with antibodies to VCIP135, p97, and p47. (D) GST–syn5ΔTM (0.5 μg) was incubated with VCIP135 (0.35 or 0.7 μg) on ice for 30 min, immobilized on glutathione beads, and washed to remove unbound VCIP135. The nucleotide-free p97/p47 (2 μg p97) was preincubated in buffer containing 1 mM nucleotides on ice for 30 min and added into the beads. After 3-h incubation at 4°C, the beads were washed and subjected to Western blotting with antibodies to VCIP135, p97, and p47. (E) p97/p47/GST–syn5ΔTM-beads and VCIP135/p97/p47/GST–syn5ΔTM-beads were prepared as in C in the presence of 1 mM AMP–PNP. Then, the beads were washed with buffer containing 5 mM AMP–PNP or ATP and incubated at 4°C for 3 h. (F) VCIP135/GST–syn5ΔTM beads were prepared as in C. p97 was added into the mixture and incubated at 4°C for 3 h. Blots were probed with antibodies to VCIP135. (G) VCIP135 (1 or 2 μg) and α-SNAP (0.1 μg) were incubated with GST–syn5ΔTM (0.4 μg) or GST (0.4 μg) on ice for 1 h and then isolated on glutathione beads. Blots were probed with antibodies to VCIP135 and α-SNAP. See also Figs. S3 and S4 available at http://www.jcb.org/cgi/content/full/jcb.200208112/DC1.

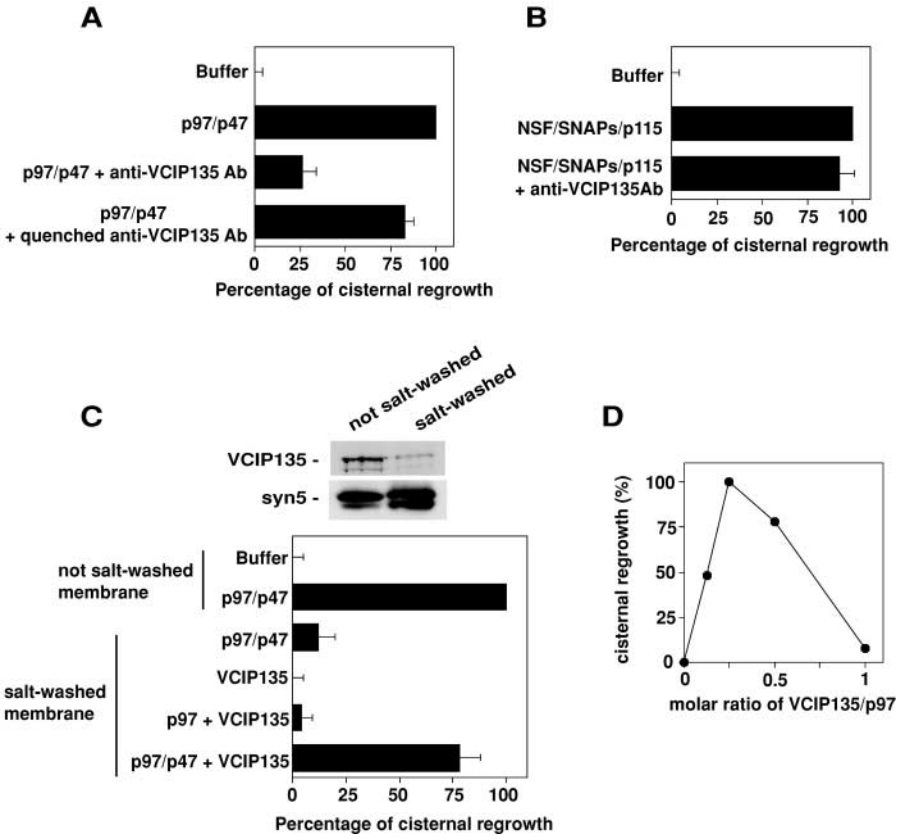

Figure 6. **VCIP135 is essential for p97/p47-mediated membrane fusion.** (A) Mitotic Golgi membranes were incubated with the indicated components at 37°C for 60 min. The membranes were fixed, processed, and the percentage of membrane in cisterna was determined. An antibody to VCIP135 was added together with the p97/p47 complex (50 μg p97/ml) to mitotic Golgi membranes. The same antibody was quenched by a VCIP135 fragment and added. Mean ± SD (n = 4); 0% represents the buffer (21.2% in cisternal membranes) and 100% represents p97/p47 alone (41.8% in cisternal membranes). (B) Antibodies to VCIP135 were added to mitotic Golgi membranes together with the components of the NSF pathway: NSF (100 μg/ml), α-SNAP (25 μg/ml), and γ-SNAP (25 μg/ml), p115 (8 μg/ml). Mean ± SD (n = 3); 0% represents the buffer (22.5% in cisternal membranes) and 100% represents NSF/SNAPs/p115 alone (40.4% in cisternal membranes). (C) The top panels show the amounts of VCIP135 in mitotic Golgi membranes and 1 M KCl-washed membranes. 1 M KCl-washed or nonwashed mitotic Golgi membranes were incubated with several components or their combinations; p97/p47 (50 μg p97/ml), VCIP135 (15 μg/ml), p97 (50 μg/ml). Mean ± SD (n = 4); 0% represents the buffer (23.2% in cisternal membranes) and 100% represents non salt-washed membranes with p97/p47 alone (43.4% in cisternal membranes). (D) 1 M KCl-washed mitotic Golgi membranes were incubated with p97/p47 (50 μg p97/ml) and several doses of VCIP135. Results are the averaged percentage (n = 3); 0% represents VCIP135/p97 = 0 (21.2% in cisternal membranes) and 100% represents VCIP135/p97 = 1/4 (44.1% in cisternal membranes).

DC1). In the presence of ATP, the addition of VCIP135 prevented p97 and p47 from binding to syntaxin5 and VCIP135 itself only bound poorly to syntaxin5 (Fig. 5 D, left three lanes). However, in the presence of AMP–PNP or ADP, p97 and p47 bound to syntaxin5 even when VCIP135 was added, and VCIP135 also bound to syntaxin5 (Fig. 5 D, right six lanes). These data suggest that both VCIP135 and the p97/p47 complex bind to syntaxin5, resulting in the formation of a transient quaternary complex that could be dissociated through p97 ATP hydrolysis. To clarify this further, we performed dissociation experiments as described in Fig. 5 E (see also Fig. S4 available at http://www.jcb.org/cgi/content/full/jcb.200208112/DC1). We initially prepared complexes of p97/p47/GST–syn5ΔTM or VCIP135/p97/p47/GST–syn5ΔTM in the presence of AMP–PNP. Both complexes were maintained under these conditions. Then, the beads containing both complexes were incubated in the presence of AMP–PNP or ATP. The p97/p47/GST–syn5ΔTM complex was maintained intact even in the presence of ATP (Fig. 5 E, lanes 1 and 2). However, the VCIP135/p97/p47/GST–syn5ΔTM complex was dissociated only in the presence of ATP (Fig. 5 E, lane 4), and the VCIP135/p97 complex was observed in the supernatant (unpublished data). This result strongly suggests that VCIP135 dissociates the p97/p47/syntaxin5 complex via ATP hydrolysis by p97.

Although VCIP135 can bind to p97 in cytosol (Fig. 3 A), VCIP135 bound to syntaxin5 does not form a complex with p97 (Fig. 5 C, lane 4). This suggests that the formation of a VCIP135/p97 complex on syntaxin5 dissociates VCIP135 from syntaxin5. To investigate this, we performed stripping experiments as shown in Fig. 5 F. p97 was added to a complex of VCIP135/GST–syn5ΔTM, and the remaining amounts of VCIP135 on GST–syn5ΔTM were determined. The addition of p97 decreased the amount of VCIP135 bound to syntaxin5 (Fig. 5 F). The dissociated VCIP135 was observed as a complex with p97 in the supernatant (unpublished data).

We also investigated whether VCIP135 has any effect on the binding of α-SNAP to syntaxin5. As shown in Fig. 5 G, VCIP135 partially prevented α-SNAP binding to GST–syn5ΔTM, suggesting that VCIP135 directs syntaxin5 to p97/p47 but not to α-SNAP/NSF.

VCIP135 is essential for p97/p47-mediated membrane fusion

We have shown that VCIP135 binds to syntaxin5 and disassembles the p97/p47/syntaxin5 complex through p97 ATP hydrolysis. Next, we wanted to ascertain whether VCIP135 contributes to p97/p47-mediated membrane fusion using an in vitro Golgi reassembly assay. As shown in Fig. 6 A, cisternal regrowth was observed by the incubation of mitotic Golgi fragments with the p97/p47 complex (the control). Anti-VCIP135 antibodies inhibited the p97/p47-mediated cisternal regrowth by ~75% compared with the control.

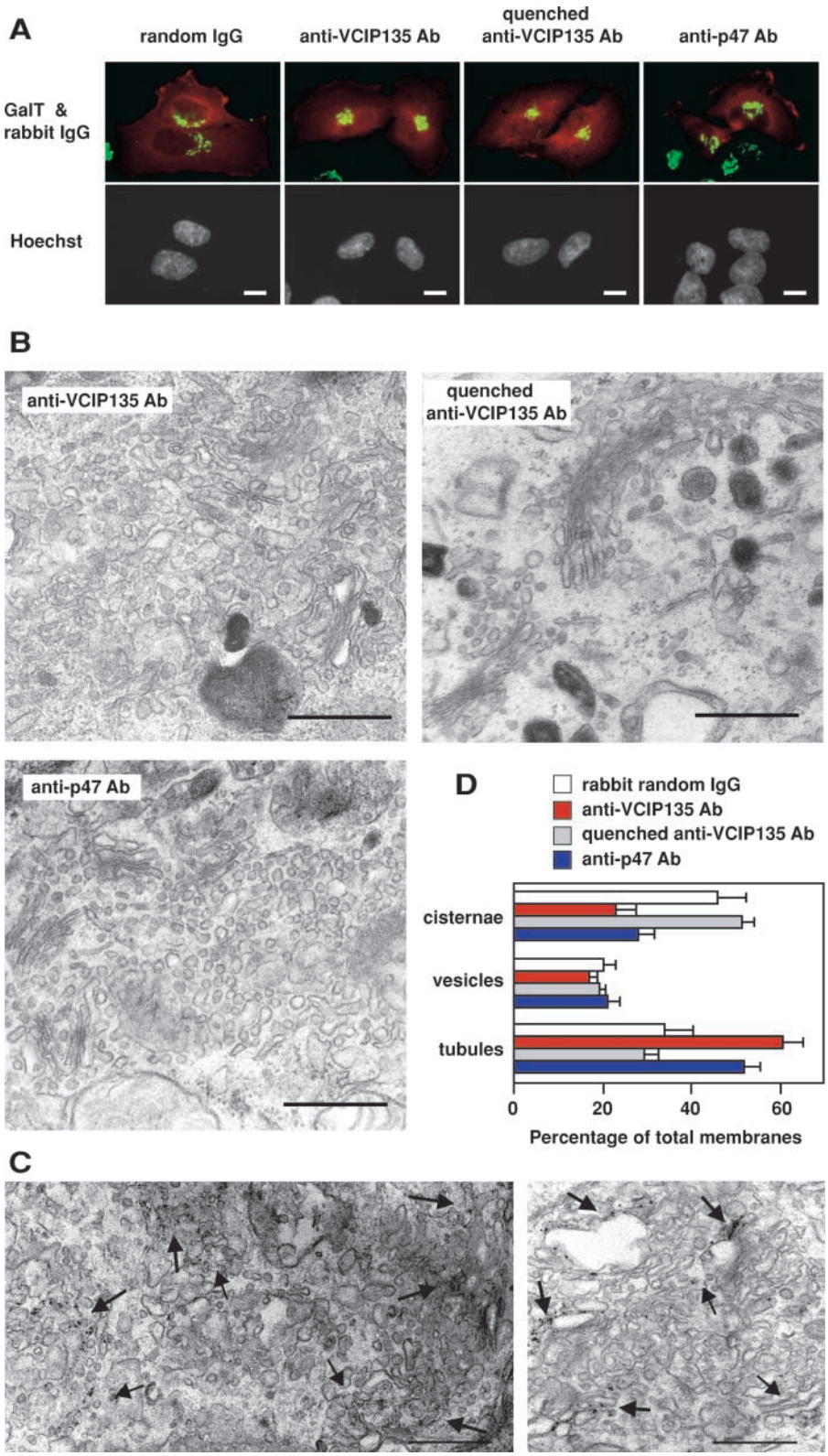

Figure 7. **VCIP135 is required for Golgi assembly in vivo.** (A) NRK cells at prophase (or early prometaphase) were injected with antibodies and fixed after they exited mitosis. Golgi (green, top), injected antibodies (red, top), and chromatin (bottom) were stained by monoclonal anti-GalT antibodies, anti–rabbit IgG antibodies, and Hoechst33342, respectively. Bars, 10 μm. (B) Representative EM images of Golgi in daughter cells after antibodies or quenched antibodies were microinjected. Bars, 0.5 μm. (C) Immunolabeling EM images of Golgi area in the NRK cells microinjected with anti-VCIP135 antibodies. For immunolabeling of Golgi marker proteins, monoclonal antibodies to either GalT (left) or GM130 (right) were used. Arrows show immunolabeled vesicles and tubules. Bars, 0.5 μm. (D) Golgi membranes were classified and counted as described previously (Shorter and Warren, 1999; Seemann et al., 2000) in microinjected cells. Mean ± SD (n = 7–9).

This inhibition was rescued by quenching the antibodies with a VCIP135 fragment. The antibodies had no effect on NSF-mediated cisternal regrowth (Fig. 6 B). Together, these results strongly suggest that VCIP135 is specifically involved in the p97/p47 membrane fusion pathway.

The above assays were performed with Golgi mitotic fragments that were contaminated by membrane-bound VCIP135. Therefore, we performed assays using VCIP135-free membranes obtained by 1 M KCl washes (Fig. 6 C, top). When the VCIP135-free membranes were incubated with p97/p47, VCIP135, or p97/VCIP135, no cisternal regrowth was observed. Only when p97/p47 and VCIP135 were added together was cisternal regrowth observed (Fig. 6 C). Thus, VCIP135 is an essential factor for p97/p47-medi-

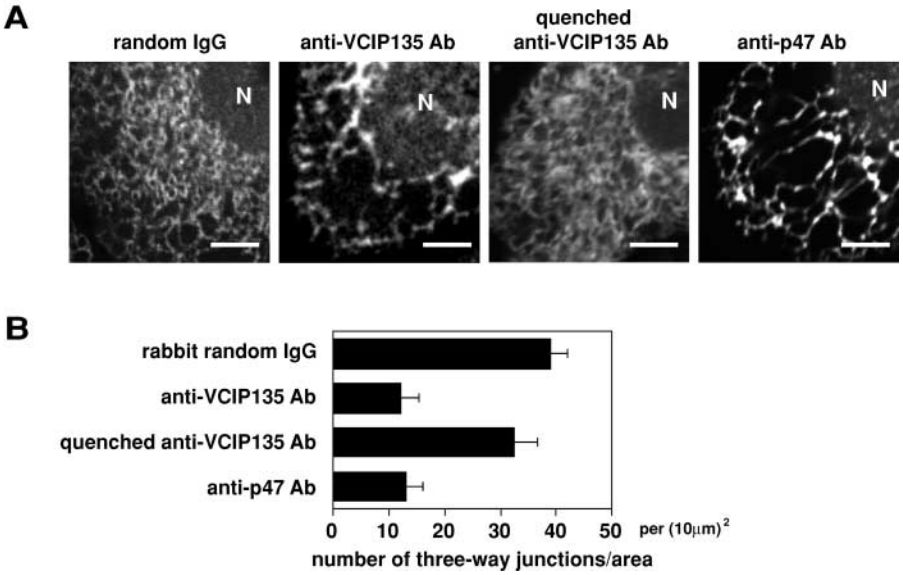

Figure 8. **VCIP135 is required for ER network formation in vivo.** (A) Antibodies were microinjected into CHO cells expressing GFP-tagged HSP47. Since ER structures were easily damaged and lost after fixation, they were observed in living cells without fixation by confocal microscopy. Representative images of ER in daughter cells after the injection of antibodies are shown. N, nucleus. Bars, 5 μm. (B) The number of three-way junctions was counted by confocal microscopy as a parameter of ER network formation. Mean ± SD (n = 9).

ated membrane fusion. Fig. 6 D shows the dose dependency of VCIP135 on cisternal regrowth. Interestingly, it is biphasic: a low level of VCIP135 (1/8–1/2 [mol/mol p97]) had a positive effect on the cisternal regrowth, whereas a higher level of VCIP135 had a negative effect.

VCIP135 is required for Golgi and ER assembly in vivo

Although many groups have reported the in vitro function of p97 in the biogenesis of organelles, its in vivo function still remains unclear. Since p97 is known to be involved in several biological processes (Patel and Latterich, 1998; Meyer et al., 2000; Dai and Li, 2001; Ye et al., 2001; Jarosch et al., 2002), a specific cofactor other than p97 would be a better target to mediate its fusion-specific function. We have now identified VCIP135 as an essential cofactor for the fusion activity of p97 in vitro. To study the function of VCIP135 in vivo, we microinjected anti-VCIP135 antibodies into cells and investigated its effects on the reassembly of organelles at the end of mitosis. Cells at prophase (or early prometaphase) were injected with anti-VCIP135 antibodies and fixed after they entered interphase. An anti-VCIP135 antibody quenched by its antigen and rabbit random IgG were injected as negative controls, and an anti-p47 antibody was used as a positive control. The injections of these antibodies had no effect on cell cycle progression.

As shown in Fig. 7 A, the Golgi was stained by mAbs to GalT, a Golgi marker (Rabouille et al., 1995a). Hoechst DNA staining showed that injected cells had exited mitosis (bottom). After the injection of either anti-VCIP135 or anti-p47 antibodies, Golgi still localized to a perinuclear region in daughter cells (top panel 2 and 4, respectively). The ultrastructure of the Golgi in injected cells was investigated by EM (Fig. 7, B–D). In anti-VCIP135 antibody-injected cells, highly organized Golgi complexes were lost: stacked cisternae were rarely observed (anti-VCIP135 antibody injection, 30.3% of cisternal membranes in stacks; random IgG injection, 80.4%), and the number of tubular/fenestrated structures was greatly increased (Fig. 7 B, top left). As shown in Fig. 7 C, immuno-EM images using antibodies to Golgi marker proteins, GalT or GM130 (Nakamura et al., 1995; Rabouille et al., 1995a), showed that these fragmented membranes were derived from Golgi. The quantitative results are shown in Fig. 7 D. The injection of anti-VCIP135 antibodies significantly decreased the percentage of cisternae per Golgi area by a half and significantly increased the percentage of tubules twofold compared with injections of quenched antibodies and random IgG. The amount of vesicles was not changed. Similar morphological changes were observed after the injection of anti-p47 antibodies (Fig. 7 B, left bottom, and D). Since the injection of the anti-VCIP135 antibodies at the same concentration into interphase cells caused no obvious changes in the organization of the Golgi apparatus (by IF and EM observation [unpublished data]), these morphological changes were most likely caused by the inhibition of reassembly at the end of mitosis. These data show that VCIP135 functions in the reassembly of highly organized Golgi structures in living cells as does p47, indicating that p97-mediated fusion is required for Golgi reassembly in living cells.

p97/p47 has also been implicated in ER membrane fusion in an in vitro system (Hetzer et al., 2001). VCIP135 localizes to ER membranes and Golgi (Fig. 4, bottom). Hence, we investigated the effect of antibodies to VCIP135 on ER structures. As shown in Fig. 8 A, the injection of anti-VCIP135 antibodies caused formation of a large meshed ER network in daughter cells (panel 2). Injection of anti-p47 antibodies had a similar effect (Fig. 8 A, panel 4). This change in ER structure was not observed after injecting quenching antibodies (Fig. 8 A, panel 3) or random IgG (panel 1). To quantify the degree of ER network formation, the number of three-way junctions was counted using confocal microscopy (Fig. 8 B). The number of three-way junctions was significantly decreased by ~70% compared with control by the injection of antibodies to VCIP135 and p47. These data indicate that the p97/p47/VCIP135 pathway also participates in ER network formation in living cells.

The structures of other organelles, including nuclear envelope, mitochondria, and lysosome, were also investigated by

EM in the antibodies injected cells. After microinjection of either anti-VCIP135 or anti-p47 antibodies, no obvious morphological changes in these organelles were observed (unpublished data) in contrast with the changes seen in the structures of the Golgi and ER. Detailed images of the cells injected with anti-VCIP135 antibodies are shown in Figs. S5 and S6, available at http://www.jcb.org/cgi/content/full/jcb.200208112/DC1.

Discussion

The p97/p47 membrane fusion pathway differs from the NSF/SNAPs pathway in that p97 catalyzed ATP hydrolysis does not dissociate the p97/p47/SNARE complex. To explain these apparent functional differences, we developed a model for p97/p47 action that would require another factor to dissociate the p97/p47/SNARE complex, presumably as part of the SNARE priming process. We postulated that this factor would interact with the p97/p47 complex and tried to isolate it. We first found two distinct binding interactions for the p97/p47 complex and based on this mapping information identified a novel protein VCIP135 from cytosol. VCIP135 dissociates the p97/p47/syntaxin5 complex via p97 catalyzed ATP hydrolysis and is shown to be essential for p97/p47-mediated membrane fusion.

In cytosol, we have shown that VCIP135 dissociates p97 from a p97/p47 complex by forming a complex with p97: p97 is translocated from p47 to VCIP135 through p97 ATP hydrolysis (Fig. 3). We would predict a similar situation for p97/p47 bound to syntaxin5, where VCIP135 would dissociate p97 from a p97/p47/syntaxin5 complex. VCIP135 bound to syntaxin5 is thought to associate with a syntaxin5-bound p97/p47 complex with syntaxin5 acting as a scaffold for the p97/p47 dissociation reaction. Hence, we present our model to explain how VCIP135 dissociates the p97/p47/syntaxin5 complex. First, VCIP135 interacts with the p97/p47 complex on syntaxin5. p97-catalyzed ATP hydrolysis causes the translocation of p97 from p47 to VCIP135, resulting in a metastable complex of p97/VCIP135/syntaxin5. Since the p97/VCIP135/syntaxin5 complex is very unstable (Fig. 5 C), a tighter VCIP135/p97 complex then dissociates from syntaxin5 (Fig. 5 F). During this disassembly process, p47 is also dissociated from syntaxin5 (Fig. 5, D and E). p47 can bind to syntaxin5 when dissociated from p97 and present alone (Rabouille et al., 1998). VCIP135 cannot interact with p47 directly (Fig. 3 A). Hence, it is most likely that a conformational change in syntaxin5 was caused to lessen its binding affinity for p47 during this disassembly process. We have found that p97 mutants that lacked ATPase activities show no membrane fusion activities in the in vitro Golgi reassembly assay (unpublished data), indicating that p97-mediated fusion requires its ATPase activity: i.e., p97 is thought to function for the ATPase-dependent disassembly of SNAREs. Considering that the disassembly of the p97/p47/SNARE complex by VCIP135 requires ATP hydrolysis (Fig. 5 E), we suggest that the function of VCIP135 in membrane fusion is to mediate the dissociation of the p97/p47/SNARE complex, which may be part of the SNARE priming process. Recently, NSF/SNAP have been suggested to mediate the ATPase-independent SNARE assembly and the ATPase-dependent SNARE disassembly (Müller et al., 2002). It is unclear at this moment whether p97/p47/VCIP135 also have ATPase-independent functions or not. Nevertheless, further biochemical and functional investigations are necessary to clarify the mechanism and functional significance of the disassembly of the p97/p47/SNARE complex mediated by VCIP135.

The binding of VCIP135 to syntaxin5 independently of p47 (Fig. 5 C) allows VCIP135 to be closely associated with the p97/p47 complex, whereas in cytosol such an association is less likely. Accordingly, a smaller amount of VCIP135 (1/8–1/4 [mol/mol p97]) was sufficient for the disassembly of the p97/p47/syntaxin5 complex (Fig. 5 D), whereas a larger amount of VCIP135 (1/2–1 [mol/mol p97]) was necessary for the dissociation of the p97/p47 complex (Fig. 3 D). The disassembly of the p97/p47/SNARE complex works positively for membrane fusion, and the dissociation of the p97/p47 complex works negatively. This may provide a mechanism to explain the biphasic dose-dependent curve of VCIP135 in Golgi cisternal regrowth (Fig. 6 D). On the other hand, p47 has been reported to inhibit p97 ATPase activity (Meyer et al., 1998). One possible explanation for this inhibition is that p47 interacts with p97 using two distinct binding interfaces (Fig. 1) to form a tight conformationally restrictive complex that inhibits p97 ATPase activity. The inhibition of p97 ATPase activity can be reduced if both p47-binding sites are not occupied, and the metastable complex of VCIP135/p97/p47 would represent such a case: VCIP135 interacts with the p97/p47 complex that uses only one p47-binding site. The release of ATPase inhibition in this transient complex could allow the necessary ATPase activity required for p97 translocation from p47 to VCIP135.

Finally, we have clarified by microinjection of antibodies to VCIP135 and p47 that fusion-specific cofactors of p97 participate in Golgi and ER assembly (Figs. 7 and 8). This is the first report to show p97-mediated membrane fusion in vivo. From experiments using an in vitro Golgi reassembly assay, it is suggested that p97 may mediate homotypic fusion of short tubules and larger vesicles to form unfenestrated cisternae in contrast to NSF-mediating heterotypic fusion of small vesicles (Acharya et al., 1995; Rabouille et al., 1995b). Our results are in good agreement with this. As shown in Fig. 7 D, the injection of anti-VCIP135/p47 antibodies caused accumulation of tubules, which are thought to be the starting membranes for homotypic fusion, but not vesicles, which are required for heterotypic fusion. Unfenestrated cisternae, products of homotypic fusion, were decreased by injection of anti-VCIP135/p47 antibodies (Fig. 7, B and D). These in vivo data strongly support the hypothesis that p97 mediates homotypic fusion. Moreover, the injection of anti-VCIP135/p47 antibodies inhibited stack formation as well as cisternal regrowth (Fig. 7 B), which is consistent with the previous observation in semiintact cells (Acharya et al., 1995). One possible explanation is that stack formation may require growth of unfenestrated cisternae mediated by p97: the extended and smooth surfaces of cisternae could give each individual cisterna more opportunities to meet another one for stacking.

In this paper, we report that, similar to NSF/SNAPs, p97/p47 is dissociated from the SNARE through p97-mediated ATP hydrolysis. The dissociation of p97/p47 from the SNARE differs from that of NSF/SNAP in that p97/p47 requires the assistance of another essential factor, VCIP135. We are now focusing on whether p97, p47, and VCIP135 are necessary and sufficient for the priming of SNAREs and determining the underlying mechanism.

Materials and methods

Proteins and antibodies

NSF, SNAPs, p47, and GST–syn5ΔTM were prepared as described previously (Rabouille et al., 1995b, 1998; Kondo et al., 1997). p115 and p97 were purified from rat liver cytosol (Rabouille et al., 1995b; Kondo et al., 1997). Rat p97 cDNA was PCR amplified from a rat liver cDNA library and subcloned into pTrcHisB. To obtain GST-tagged and His-tagged deletion mutants of p97 and p47, the corresponding cDNAs with stop codons were subcloned into pGEX4T-2 and pQE30, respectively. mAbs to PDI and GalT were gifts from Dr. Vaux (Oxford University, Oxford, UK) and Dr. Suganuma (Miyazaki Medical College, Miyazaki, Japan), respectively. Monoclonal antibodies to p97, His tag, and GM130 were purchased from Progen, QIAGEN, and BD Transduction, respectively.

Purification of VCIP135

His-p47(171–270) and His-p47(271–370) (100 μg each) were biotinylated using EZ-Link Sulfo-NHS-LC-biotin (Pierce Chemical Co.), bound to immobilized NeutrAvidin plus beads (Pierce Chemical Co.), and washed with 1 M KCl in buffer A (20 mM Hepes, 1 mM $MgCl_2$, 1 mM ATP, 1 mM DTT, 0.1% Triton X-100, 10% glycerol, pH 7.4). Rat liver cytosol (65 mg total protein), which was supplied with KCl (to 1 M) and Triton X-100 (to 0.1%), was incubated with the resulting beads for 1 h at 4°C. The mixtures were diluted to 0.15 M KCl with buffer A and incubated for 2 h at 4°C. The binding proteins were eluted with 1 M KCl in buffer A, subjected to trichloroacetic acid precipitation, and separated by SDS-PAGE.

Cloning of VCIP135 cDNA

The Zn-stained protein band was excised from the gel and subjected to protein microsequencing as described previously (Meyer et al., 2000). From the protein microsequencing, we obtained two partial peptide sequences: peptide 1, QL(I)DPDVVEAQR and peptide 2, QEEL(I)AVTGK. An EST database search showed one rat cDNA clone (EST236550) that contained a corresponding cDNA sequence to peptide 1. An identical clone was isolated by PCR from a rat liver cDNA library. Pfu Turbo (Stratagene) was used as DNA polymerase. This clone was sequenced to confirm that it encoded peptide 1. Since this clone had a stop codon in the reading frame, its cDNA sequence was extended to the 5′-end with a Marathon cDNA Amplification kit (CLONTECH Laboratories, Inc.) (gene specific primer, 5′-TGATGCCTGAATAGAAGAAACCATTTCCTGC-3′ and nested primer, 5′-CTCAACCACATCGGGATCAATCTGCCTACC-3′). We obtained four independent clones of ∼2.3 kbp and determined their sequences. The sequences of all the clones were identical, and they encoded peptide 2. The second 5′-RACE was performed to extend further to the 5′-end (gene-specific primer, 5′-CTCCACGCAATACAGATTGGCTTGTTC-3′ and nested primer, 5′-AAATGACCATCTCTCCCAGTGCAC-3′). Three independent clones of 1.1–1.05 kbp covered the 5′-end, and all had identical sequences. Finally, the entire cDNA of 3,804 bp was reisolated directly from rat liver cDNA library by PCR and resequenced. Its start codon was confirmed using an in vitro transcription/translation system (Promega).

After mutating the BamHI sites in the ORF of VCIP135 without changing the encoded amino acid sequence, it was subcloned into pTrcHisB using BamHI and EcoRI sites. Recombinant VCIP135 was expressed in *Escherichia coli* and purified with Ni beads followed by further purification with gel filtration and 5–30% sucrose-gradient sedimentation. His-tagged VCIP135(744–1221) was used to raise rabbit anti-VCIP135 polyclonal antibodies.

Binding experiments with purified proteins

Binding experiments with GST–syn5ΔTM were performed using buffer A containing 0.15 M KCl, 0.5 mg/ml trypsin inhibitor, and 0.1% deoxycholic acid instead of 0.1% Triton X-100. For all other binding experiments, 0.1% Triton X-100 was used. GST-tagged proteins and their interacting partners were precipitated by glutathione-Sepharose. His-tagged proteins were precipitated using anti-His antibodies and protein A–Sepharose.

Sucrose-gradient sedimentation

Rat liver cytosol was loaded onto a 5–30% sucrose gradient (containing 0.1 M KCl, 20 mM Hepes, 1 mM $MgCl_2$, 1 mM ATP and 1 mM DTT, pH 7.4) and centrifuged for 5 h at 55,000 rpm in a TLS-55 rotor (Beckman Coulter). 12 fractions were collected from the top.

Immunoprecipitation from rat liver cytosol

Rat liver cytosol (3.5 mg total protein) was mixed with anti-VCIP135 antibodies in buffer A containing 0.15 M KCl. VCIP135 and its binding proteins were immunoprecipitated by protein A beads. Preimmune serum was used as a control.

For the immunoprecipitation experiment using anti-p47 antibodies, a cross-linker reagent, SAND (Pierce Chemical Co.), was added to rat liver cytosol (pH 7.4) and photoactivated by a 5 min exposure to UV light (365 nm). The cross-linking reaction was quenched by the addition of Tris (pH 7.4) to 0.1 M, and the cytosol was then subjected to immunoprecipitation by anti-p47 antibodies.

Immunoprecipitation from membranes

Golgi membranes were purified from rat liver (Hui et al., 1998). 1 M KCl-washed membranes (150 μg) were incubated with His-tagged VCIP135 (2 μg) in buffer (40 mM Hepes, 0.15 M KCl, 1 mM $MgCl_2$, 0.2 M sucrose, pH 7.4) for 1 h at 4°C. The membranes were recovered by centrifugation and solubilized in buffer (40 mM Hepes, 0.15 M KCl, 1 mM $MgCl_2$, 1 mM DTT, 10% glycerol, 1% CHAPS, protease inhibitor cocktail [Roche], pH 7.4). Monoclonal anti-His antibodies were added together with anti–mouse IgG-conjugated Dynabeads (Dynal). After incubated for 3 h at 4°C, the beads were washed and subjected to Western blotting with anti–syntaxin5 peptide antibodies.

Negative staining

Negative staining was performed as described previously (Kondo et al., 1997). 550 individual images of the end-on–oriented complexes were averaged and sixfold rotationally symmetrized.

In vitro Golgi reassembly assay

The in vitro Golgi reassembly assay was performed as reported previously (Shorter and Warren, 1999). For the preparation of salt-washed membranes, KCl was added into the mixture to 1 M, incubated on ice for 30 min, and the membranes were recovered by centrifugation. All components added in this assay were prepared as recombinant proteins from *E. coli*.

Microinjection of antibodies into living cells

Affinity-purified antibodies (∼8 μg/μl) were microinjected into prophase (or early prometaphase) NRK cells. The cells were fixed 1.5 h after injection and stained to allow visualization of the Golgi complex. For observation of ER structure, we used a stable cell line expressing GFP-tagged HSP47, an ER protein (Nagata, 1998), whose localization to ER was confirmed by immunofluorescence staining using anti-PDI antibodies. ER structures were observed in living cells, without fixation, using confocal microscopy.

For EM study, NRK cells were roughly synchronized. Cells were cultured for 12 h in presence of aphidicolin (2.5 mg/l). After washing out aphidicolin, they were cultured for 6 h and microinjected. Cells were grown on a coverslip on which a square area of ∼1 mm × 1 mm was outlined by a diamond pen. All prophase (or early prometaphase) cells within the area were injected; all injections were done within 5–10 min. Uninjected cells within the area were completely removed by an injection needle. Fluorescence of coinjected Cy3–BSA (∼1 μg/μl) was used as an indicator to distinguish injected cells from uninjected cells. The cells were fixed 1.5 h after injection. Before fixation, undivided cells within the area were completely removed by an injection needle. After fixation and embedding into Epon, the cells within the area were ultrathin sectioned (Seemann et al., 2000). The Golgi area was defined by the boundary enclosing the Golgi stacks, tubules, and tubulo-reticular networks, and all the vesicles that were within 100 nm of these membranes. Membrane profiles in the Golgi area were divided into three categories: cisternae, tubules, and vesicles, and the relative proportion of each category of membranes was counted using an intersection method as described previously (Shorter and Warren, 1999).

Immuno-EM

For immunolabeling, cells were fixed with PLP fixative (2% formaldehyde, 0.01 M periodatem, 0.075 M lysine–HCl in 0.075 M phosphate buffer, pH 7.4) for 2 h at RT. Cells were permeabilized with 0.01% saponin (Sigma-

Aldrich) and immunolabeled using anti-GalT or anti-GM130 mAbs and 1.4 nm gold particle–conjugated Fab′-fragments against mouse IgM + IgG (Nanoprobes). Nanogold was silver enhanced using HQ Silver kit (Nanoprobes) for 0.5 to 4 min and gold toned with 0.05% gold chloride (Arai et al., 1992). After washing, the cells were processed for epon embedding as above.

Online supplemental material

Online supplemental figures are available at http://www.jcb.org/cgi/content/full/jcb.200208112/DC1. Fig. S1 shows the mapping data on a VCP135-binding region in p97. Fig. S2 presents the immunoprecipitation results indicating the p47/syntaxin5/VCIP135 complex. The quantitation results of Fig. 5, D and E, are shown in Figs. S3 and S4, respectively. Figs. S5 and S6 show the detailed images of the cells injected with anti-VCIP135 antibodies.

We would like to thank M. Lindman for her excellent technical assistance on EM, T. Suganuma and J. Hay for their kind gifts of antibodies, T. Oyama (Eppendorf Japan) for his kind assistance in setting up the microinjection system, M. Lindsay, A. Stewart, and S. Arden for their kind advice and assistance, and M. Seaman, H. Davidson, and N. Nakamura for critically reading the manuscript. Special thanks to P. Luzio, K. Maruyama, and G. Warren for their kind support and encouragement.

This work was supported by a Wellcome Trust grant to H. Kondo.

Submitted: 19 August 2002
Revised: 22 October 2002
Accepted: 23 October 2002

References

Acharya, U., R. Jacobs, J.M. Peters, N. Watson, M.G. Farquhar, and V. Malhotra. 1995. The formation of Golgi stacks from vesiculated Golgi membranes requires two distinct fusion events. *Cell.* 82:895–904.

Arai, R., M. Geffard, and A. Calas. 1992. Intensification of labelings of the immunogold silver staining method by gold toning. *Brain Res. Bull.* 28:343–345.

Bayer, P., A. Arndt, S. Metzger, R. Mahajan, F. Melchior, R. Jaenicke, and J. Becker. 1998. Structure determination of the small ubiquitin-related modifier SUMO-1. *J. Mol. Biol.* 280:275–286.

Check, E. 2002. Will the real Golgi please stand up. *Nature.* 416:780–781.

Dai, R.M., and C.C. Li. 2001. Valosin-containing protein is a multi-ubiquitin chain-targeting factor required in ubiquitin-proteasome degradation. *Nat. Cell Biol.* 3:740–744.

Hetzer, M., H.H. Meyer, T.C. Walther, D. Bilbao-Cortes, G. Warren, and I.W. Mattaj. 2001. Distinct AAA-ATPase p97 complexes function in discrete steps of nuclear assembly. *Nat. Cell Biol.* 3:1086–1091.

Hui, N., N. Nakamura, B. Sonnichsen, D.T. Shima, T. Nilsson, and G. Warren. 1997. An isoform of the Golgi t-SNARE, syntaxin 5, with an endoplasmic reticulum retrieval signal. *Mol. Biol. Cell.* 8:1777–1787.

Hui, N., N. Nakamura, P. Slusarewicz, and G. Warren. 1998. Purification of rat liver golgi stacks. *In* Cell Biology: A Laboratory Handbook. Vol. 2. J. Celis, editor. Academic Press, Orlando, FL. 46–55.

Jarosch, E., C. Taxis, C. Volkwein, J. Bordallo, D. Finley, D.H. Wolf, and T. Sommer. 2002. Protein dislocation from the ER requires polyubiquitination and the AAA-ATPase Cdc48. *Nat. Cell Biol.* 4:134–139.

Jokitalo, E., N. Cabrera-Poch, G. Warren, and D.T. Shima. 2001. Golgi clusters and vesicles mediate mitotic inheritance independently of the endoplasmic reticulum. *J. Cell Biol.* 154:317–330.

Kondo, H., C. Rabouille, R. Newman, T.P. Levine, D. Pappin, P. Freemont, and G. Warren. 1997. p47 is a cofactor for p97-mediated membrane fusion. *Nature.* 388:75–78.

Latterich, M., K.U. Frohlich, and R. Schekman. 1995. Membrane fusion and the cell cycle: Cdc48p participates in the fusion of ER membranes. *Cell.* 82: 885–893.

Lucocq, J.M., E.G. Berger, and G. Warren. 1989. Mitotic Golgi fragments in HeLa cells and their role in the reassembly pathway. *J. Cell Biol.* 109:463–474.

Meyer, H.H., H. Kondo, and G. Warren. 1998. The p47 co-factor regulates the ATPase activity of the membrane fusion protein, p97. *FEBS Lett.* 437:255–257.

Meyer, H.H., J.G. Shorter, J. Seemann, D. Pappin, and G. Warren. 2000. A complex of mammalian ufd1 and npl4 links the AAA-ATPase, p97, to ubiquitin and nuclear transport pathways. *EMBO J.* 19:2181–2192.

Müller, J.M., J. Shorter, R. Newman, K. Deinhardt, Y. Sagiv, Z. Elazar, G. Warren, and D.T. Shima. 2002. Sequential SNARE disassembly and GATE-16–GOS-28 complex assembly mediated by distinct NSF activities drives Golgi membrane fusion. *J. Cell Biol.* 157:1161–1173.

Nagase, T., M. Nakayama, D. Nakajima, R. Kikuno, and O. Ohara. 2001. Prediction of the coding sequences of unidentified human genes. XX. The complete sequences of 100 new cDNA clones from brain which doce for large proteins in vitro. *DNA Res.* 8:85–95.

Nagata, K. 1998. Expression and function of heat shock protein 47: a collagen-specific molecular chaperone in the endoplasmic reticulum. *Matrix Biol.* 16: 379–386.

Nakamura, N., C. Rabouille, R. Watson, T. Nilsson, N. Hui, P. Slusarewicz, T.E. Kreis, and G. Warren. 1995. Characterization of a cis-Golgi matrix protein, GM130. *J. Cell Biol.* 131:1715–1726.

Patel, S., and M. Latterich. 1998. The AAA team: related ATPases with diverse functions. *Trends Cell Biol.* 8:65–71.

Rabouille, C., N. Hui, F. Hunte, R. Kieckbusch, E.G. Berger, G. Warren, and T. Nilsson. 1995a. Mapping the distribution of Golgi enzymes involved in the construction of complex oligosaccharides. *J. Cell Sci.* 108:1617–1627.

Rabouille, C., T.P. Levine, J.M. Peters, and G. Warren. 1995b. An NSF-like ATPase, p97, and NSF mediate cisternal regrowth from mitotic Golgi fragments. *Cell.* 82:905–914.

Rabouille, C., H. Kondo, R. Newman, N. Hui, P. Freemont, and G. Warren. 1998. Syntaxin 5 is a common component of the NSF- and p97-mediated reassembly pathways of Golgi cisternae from mitotic Golgi fragments in vitro. *Cell.* 92:603–610.

Roy, L., J.J. Bergeron, C. Lavoie, R. Hendriks, J. Gushue, A. Fazel, A. Pelletier, D.J. Morre, V.N. Subramaniam, W. Hong, and J. Paiement. 2000. Role of p97 and syntaxin 5 in the assembly of transitional endoplasmic reticulum. *Mol. Biol. Cell.* 11:2529–2542.

Seemann, J., E.J. Jokitalo, and G. Warren. 2000. The role of the tethering proteins p115 and GM130 in transport through the Golgi apparatus in vivo. *Mol. Biol. Cell.* 11:635–645.

Shorter, J., and G. Warren. 1999. A role for the vesicle tethering protein, p115, in the post-mitotic stacking of reassembling Golgi cisternae in a cell-free system. *J. Cell Biol.* 146:57–70.

Sollner, T., S.W. Whiteheart, M. Brunner, H. Erdjument-Bromage, S. Geromanos, P. Tempst, and J.E. Rothman. 1993. SNAP receptors implicated in vesicle targeting and fusion. *Nature.* 362:318–324.

Warren, G. 1993. Membrane partitioning during cell division. *Annu. Rev. Biochem.* 62:323–348.

Wickner, W., and A. Haas. 2000. Yeast homotypic vacuole fusion: a window on organelle trafficking mechanisms. *Annu. Rev. Biochem.* 69:247–275.

Ye, Y., H.H. Meyer, and T.A. Rapoport. 2001. The AAA ATPase Cdc48/p97 and its partners transport proteins from the ER into the cytosol. *Nature.* 414: 652–656.

Yuan, X., A. Shaw, X. Zhang, H. Kondo, J. Lally, P.S. Freemont, and S. Matthews. 2001. Solution structure and interaction surface of the C-terminal domain from p47: a major p97-cofactor involved in SNARE disassembly. *J. Mol. Biol.* 311:255–263.

Zaal, K.J., C.L. Smith, R.S. Polishchuk, N. Altan, N.B. Cole, J. Ellenberg, K. Hirschberg, J.F. Presley, T.H. Roberts, E. Siggia, et al. 1999. Golgi membranes are absorbed into and reemerge from the ER during mitosis. *Cell.* 99:589–601.